Visual Journey through Tuberous Sclerosis Complex: Multisystem Imaging Insights

Thiagarajan Veerappan[1*], Geetha Ganesan[1], Kalpana Sivalingam[1]

[1]Barnard Institute of Radiology, Madras Medical College, Chennai, Tamil Nadu, India

Swiss Journal of Radiology and Nuclear Medicine - www.sjoranm.com - Rosenweg 3 in CH-6340 Baar, Switzerland

Abstract

Tuberous sclerosis complex (TSC) is a rare genetic disorder affecting several systems, characterized by hamartomatous lesions in the brain, kidneys, lungs, skin, and bones. Imaging plays a pivotal role in diagnosis and management. We report a case series of four patients exhibiting diverse clinical manifestations who received multimodality imaging from 2022 to 2024. The imaging findings were aligned with clinical and diagnostic criteria established by the 2012 International TSC Consensus guidelines. The cases had distinctive radiological characteristics of TSC, encompassing subependymal nodules, subependymal giant cell astrocytomas (SEGAs), renal angiomyolipomas, pulmonary lymphangioleiomyomatosis (LAM), cutaneous lesions, and skeletal anomalies. Cross-sectional imaging facilitated precise diagnosis and directed therapies, including embolization, for renal pseudoaneurysms. The series highlights the significance of a thorough imaging strategy in recognizing both typical and incidental characteristics of TSC. Prompt identification enables swift diagnosis, focused treatment, and long term surveillance.

Keywords: Tuberous sclerosis complex; Subependymal giant cell astrocytoma (SEGA); Renal angiomyolipoma; Lymphangioleiomyomatosis (LAM); Cardiac rhabdomyoma; Neurocutaneous syndrome.

*Corresponding author: Thiagarajan Veerappan - received: 10.12.2025 - peer reviewed, accepted and published: 31.01.2026

Introduction

Tuberous sclerosis complex (TSC), also known as Bourneville disease is a rare autosomal dominant neurocutaneous disorder characterized by the development of benign hamartomatous lesions in multiple organ systems, including the central nervous system (CNS), kidneys, lungs, heart, and skin (1). It results from mutations in either the TSC1 or TSC2 genes, which encode the proteins hamartin and tuberin, respectively—both key regulators of the mammalian target of rapamycin (mTOR) signaling pathway. Dysregulation of this pathway leads to abnormal cell proliferation and differentiation, contributing to the diverse clinical and imaging manifestations of the disease (2).

TSC has an estimated incidence of approximately 1 in 6,000 to 1 in 10,000 live births and affects both sexes equally (3). The disorder exhibits complete penetrance but variable expressivity, resulting in a wide spectrum of clinical severity even among individuals within the same family. The clinical presentation of TSC is highly variable, ranging from neurologic symptoms such as epilepsy and intellectual disability to renal, pulmonary, and cardiac complications. Even the classic clinical Vogt's triad is seen in less than 50% cases only (4). Due to its multisystem involvement and phenotypic variability, imaging plays a central role not only in the initial diagnosis but also in long-term surveillance and management.

This case series aims to highlight the imaging spectrum of TSC through four representative cases, each demonstrating various manifestations across multiple organ systems. By correlating imaging findings with clinical data and current literature, this series underscores the pivotal role of radiology in the diagnosis, follow-up, and multidisciplinary care of patients with TSC.

Materials and Methods

This case series includes four patients who underwent multimodality imaging evaluation at our institution between 2022 and 2024. Diagnosis was based on established clinical and/or genetic criteria in accordance with the 2012 International Tuberous Sclerosis Complex Consensus Conference guidelines (Table 1) (5). Written informed consent was obtained from all the patients. As this was a retrospective case series using anonymized data, institutional review board (IRB) approval was waived.

Case Presentations

Case 1

A 29-year-old female arrived at the casualty with left-sided flank pain and haematuria. She was conscious with a feeble pulse, tachycardia (PR 108/min) and hypotension (BP 100/60 mmHg). She had a diffusely tender mass over the left lumbar area. After initial stabilisation, she was referred for a contrast-enhanced computed tomography (CECT) scan of the abdomen, which identified a large lesion originating from the lower pole of the left kidney characterized by an enhancing soft-tissue component, regions of fatty attenuation and anomalously dilated vascular channels (Fig. 1a-b). A rounded contrast-filled out-pouching was observed at the centre of the lesion, corresponding to a large pseudoaneurysm originating from the accessory left renal artery that supplies the lower pole of the mass (Fig. 1c-d). A comparable large lesion featuring multiple small intrarenal aneurysms was also observed in the right kidney. The abdominal findings suggested bilateral renal angiomyolipomas (AMLs). The investigation was expanded to incorporate computed tomography (CT) imaging of the brain which revealed multiple calcified subependymal nodules (SENs) (Fig. 1e). The clinical examination also showed multiple dark papulonodular lesions over her face (Fig. 1f). A diagnosis of TSC was made based on three major features. The patient was then transferred to the Digital Subtraction Angiography (DSA) suite for urgent endovascular management. Selective catheterisation of the left lower pole renal artery showed a large pseudoaneurysm arising from the distal branch which was then subsequently treated with coiling (Fig. 1g-i).

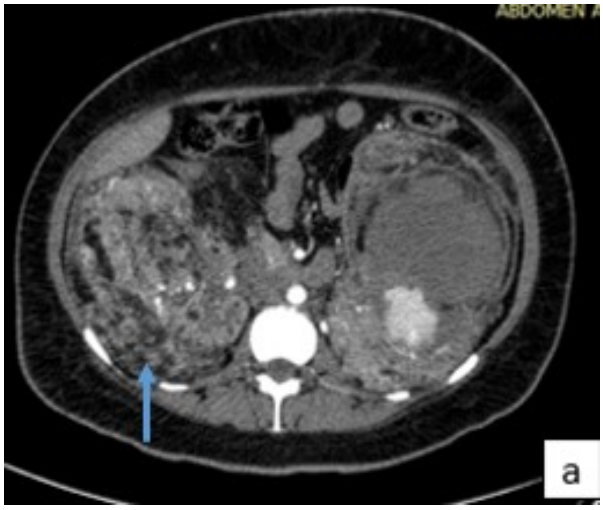

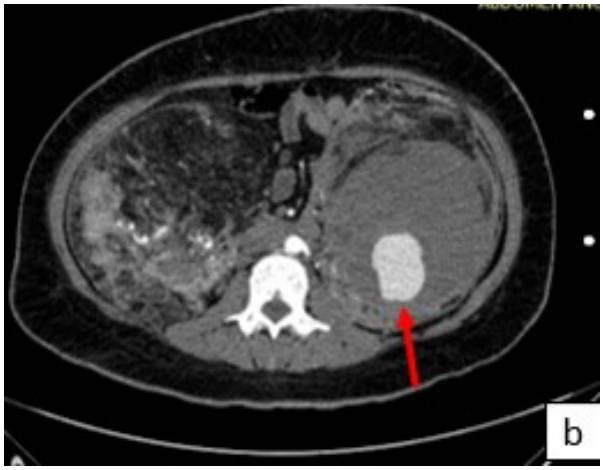

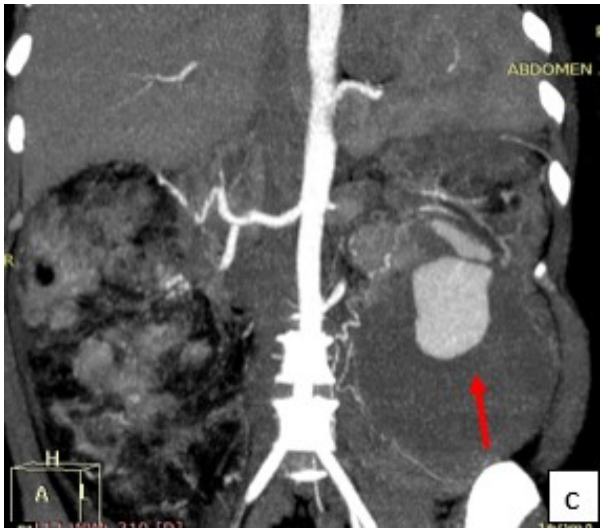

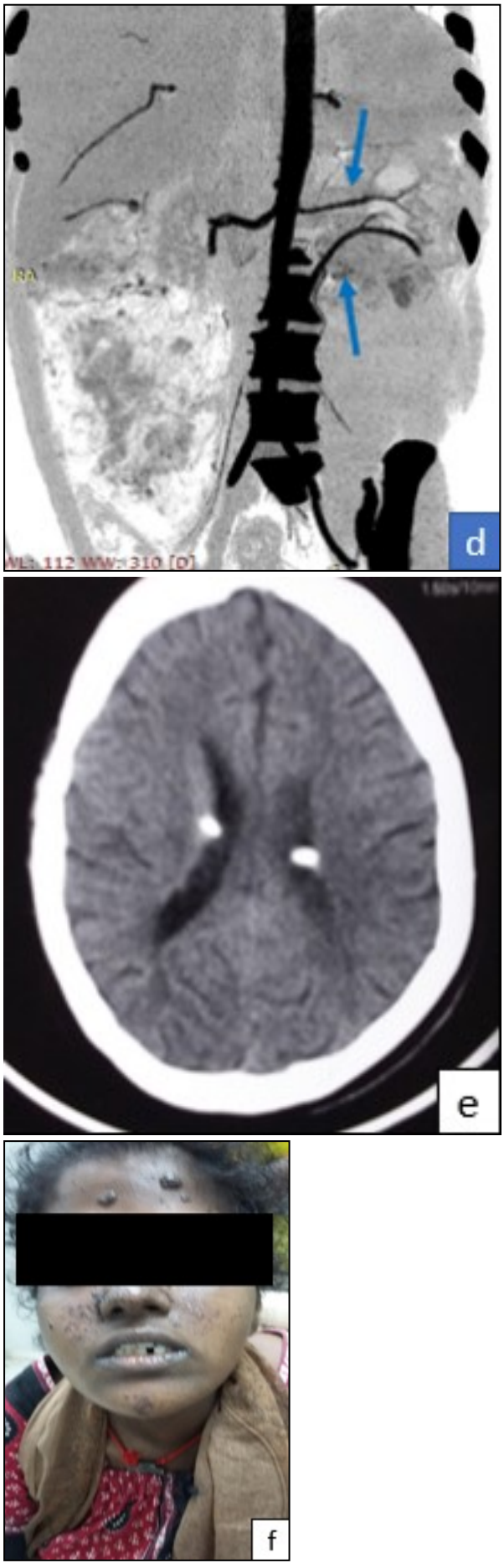

Fig. 1 a) – CECT abdomen showing well marginated heterogenous tumor predominantly fat density of size 23 x 12 x 10 cm arising from the right kidney and extending up to right iliac fossa (blue arrow) **b)** Another similar mass lesion of size 24 x 12 x 11 cm noted arising from the lower pole of left kidney with large pseudoaneurysm within (red arrow). **c, d)** – angiogram MIP images showing normal abdominal aorta and double left renal artery (blue arrows). Upper left renal artery appear normal and lower one at L3 level displaced by mass and pseudoaneurysm arising from the distal branch (red arrow). Right renal artery of normal calibre with multiple small aneurysms seen arising from the intra renal branches **e)** – CT brain image showing multiple calcified subependymal nodules **f)** – Clinical image of face of the patient showing multiple angiofibromas **g)** – DSA image showing large pseudoaneurysm arising from the distal branch of left lower pole renal artery (red arrow), **h)** – after coiling of the feeder vessel, no contrast filling of pseudoaneurysm, **i)** – Multiple intrarenal aneurysms arising from the right renal artery (blue arrow).

Case 2

A 19-year-old female presented with new-onset seizures accompanied by persistent vomiting for one week. She also reported a two-month history of progressive headaches. On physical examination, multiple facial angiofibromas were noted (Fig. 2a), raising clinical suspicion for a neurocutaneous syndrome.

Magnetic resonance imaging (MRI) of the brain revealed an ill-defined T2/FLAIR hyperintense lesion arising from the septum pellucidum and extending into the anterior horn of the right lateral ventricle and the foramen of Monro. The lesion demonstrated internal blooming foci on susceptibility-weighted imaging and avid enhancement following contrast administration—imaging features consistent with a subependymal giant cell astrocytoma (SEGA) (Fig. 2b-g).

Given these findings, further systemic evaluation was undertaken. Abdominal ultrasonography and contrast-enhanced CT revealed multiple bilateral renal angiomyolipomas (Fig. 2h-i). Additionally, skeletal window imaging demonstrated several discrete sclerotic bone lesions (bone islands) (Fig. 2j-k). Based on the fulfillment of three major diagnostic criteria, a definitive diagnosis of TSC was established.

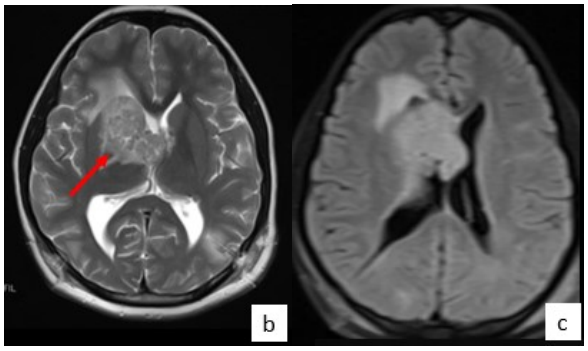

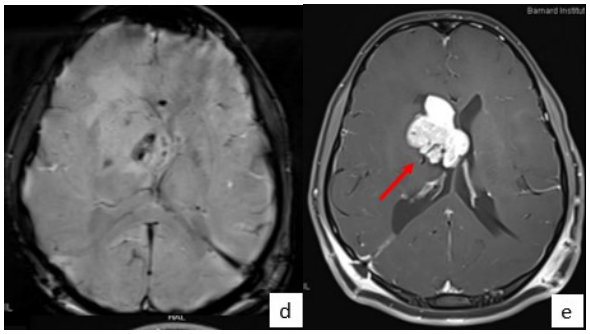

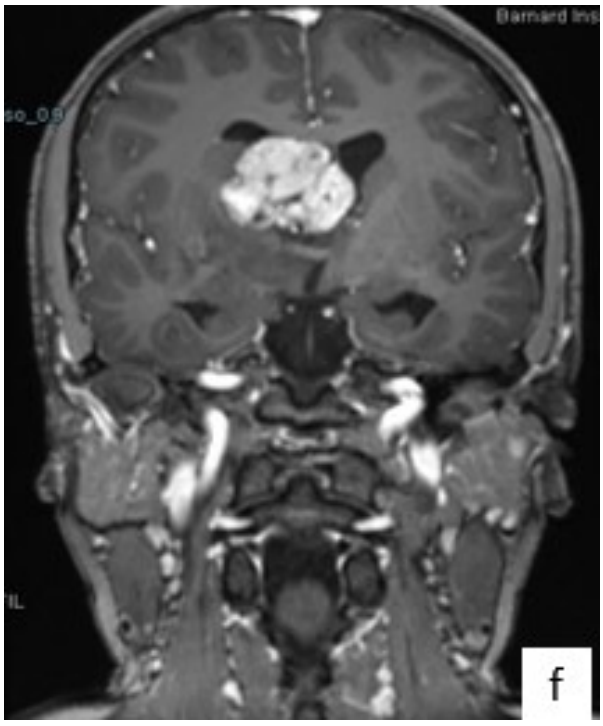

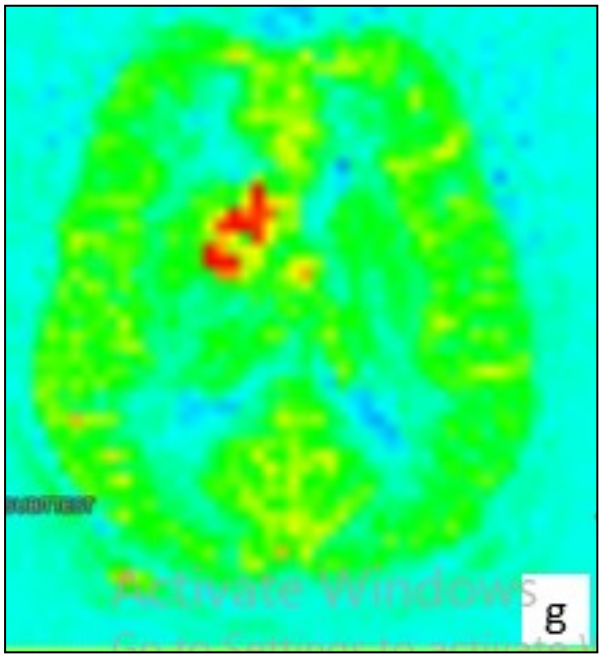

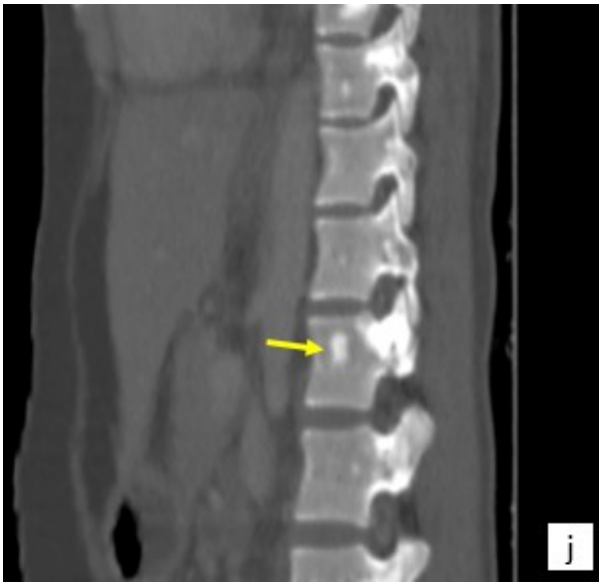

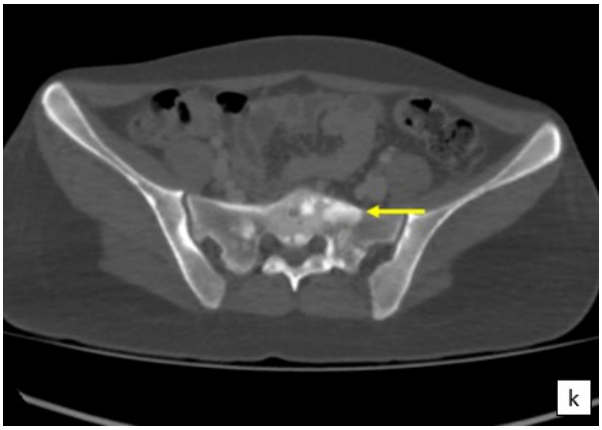

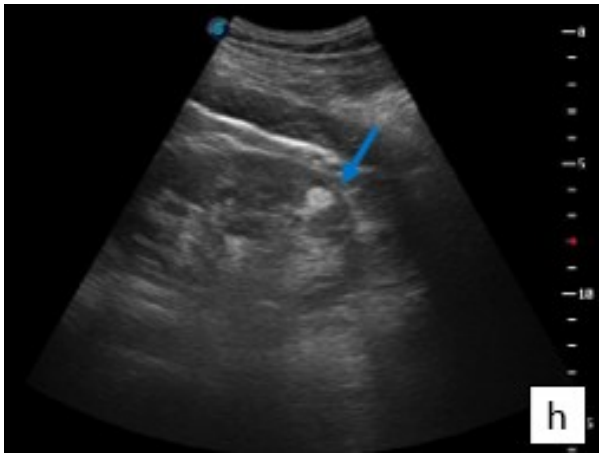

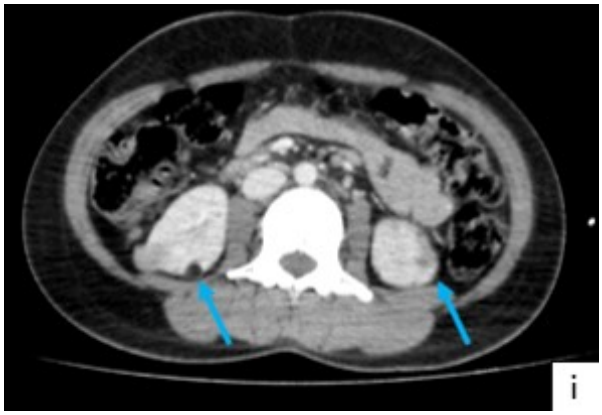

Fig. 2 a) – Clinical image of the patient's face revealing angiofibromas **b, c)** - MRI images showing an ill defined T2/Flair hyperintense lesion (red arrow) measuring 3.1 x 2.8 x 2.5 cm showing internal gradient blooming **d)** with avid contrast enhancement (red arrow) **e,f)** and increased perfusion **g)** noted arising from the septum pellucidum and extending into the right foramen of monro, consistent with SEGA. **h, i)** – USG and CECT of the abdomen showing multiple bilateral small renal angiomyolipomas (blue arrow). **j, k)** – multiple bone islands noted in dorsal vertebra and in pelvis (yellow arrow)

Case 3

A 32-year-old female with a known history of seizure disorder on regular medication presented with abdominal pain for one week. An initial abdominal ultrasound at an outside facility revealed a large heterogeneous mass arising from the left kidney. MRI of the abdomen showed a large T2 heterointense solid-cystic lesion with predominant solid components arising from the lower pole of the left kidney, displacing adjacent bowel loops. Gradient sequences demonstrated multiple blooming foci suggestive of haemorrhage, and the lesion exhibited peripheral

diffusion restriction. Post-contrast images revealed peripheral heterogeneous enhancement with central non-enhancing areas (Fig. 3a-f). A similar but smaller lesion was noted in the mid-pole of the right kidney. Screening CT confirmed the presence of fat within both lesions, consistent with renal AMLs (Fig. 3g). A subsequent CT chest demonstrated diffuse ground-glass opacities with scattered thin-walled cysts, suggestive of pulmonary lymphangioleiomyomatosis (LAM) (Fig. 3h-i) and a CT brain revealed multiple calcified SENs (Fig. 3j). Based on these findings, a diagnosis of tuberous sclerosis complex was established.

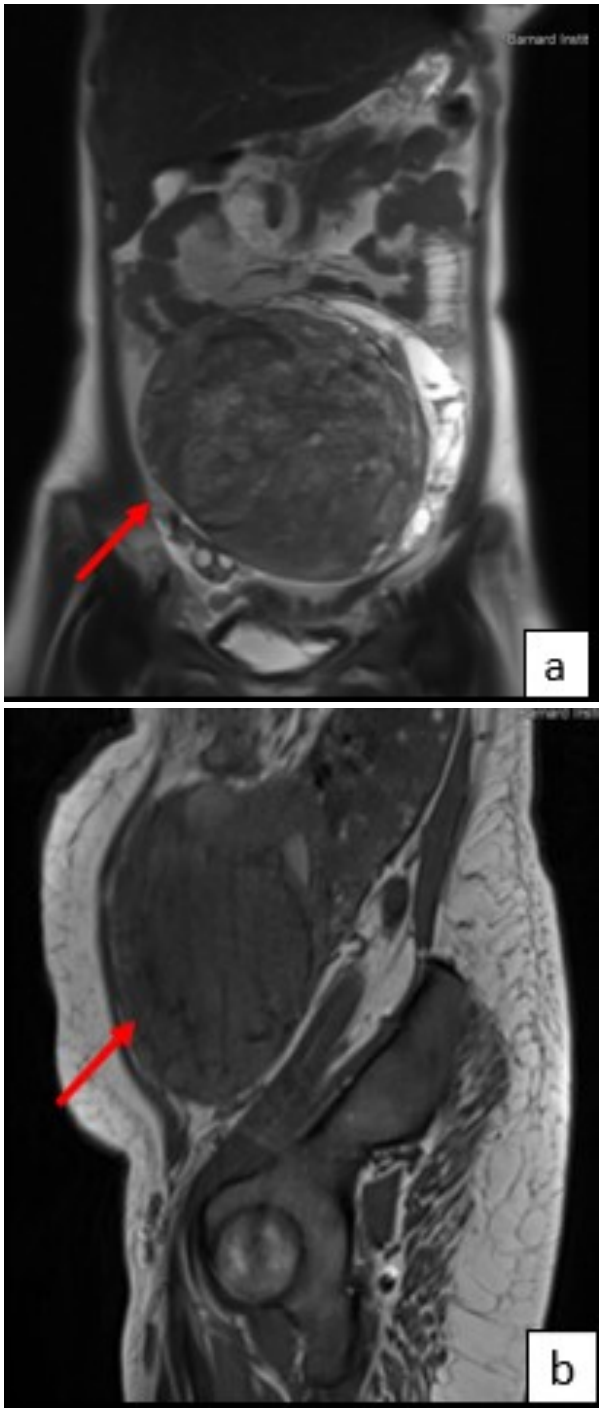

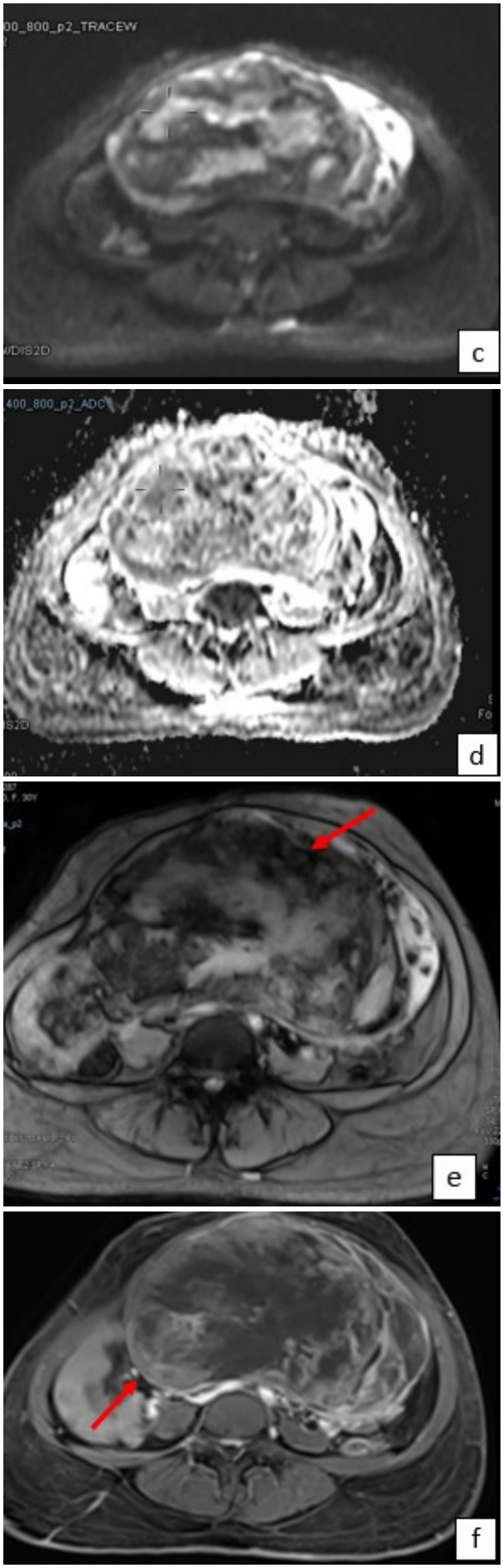

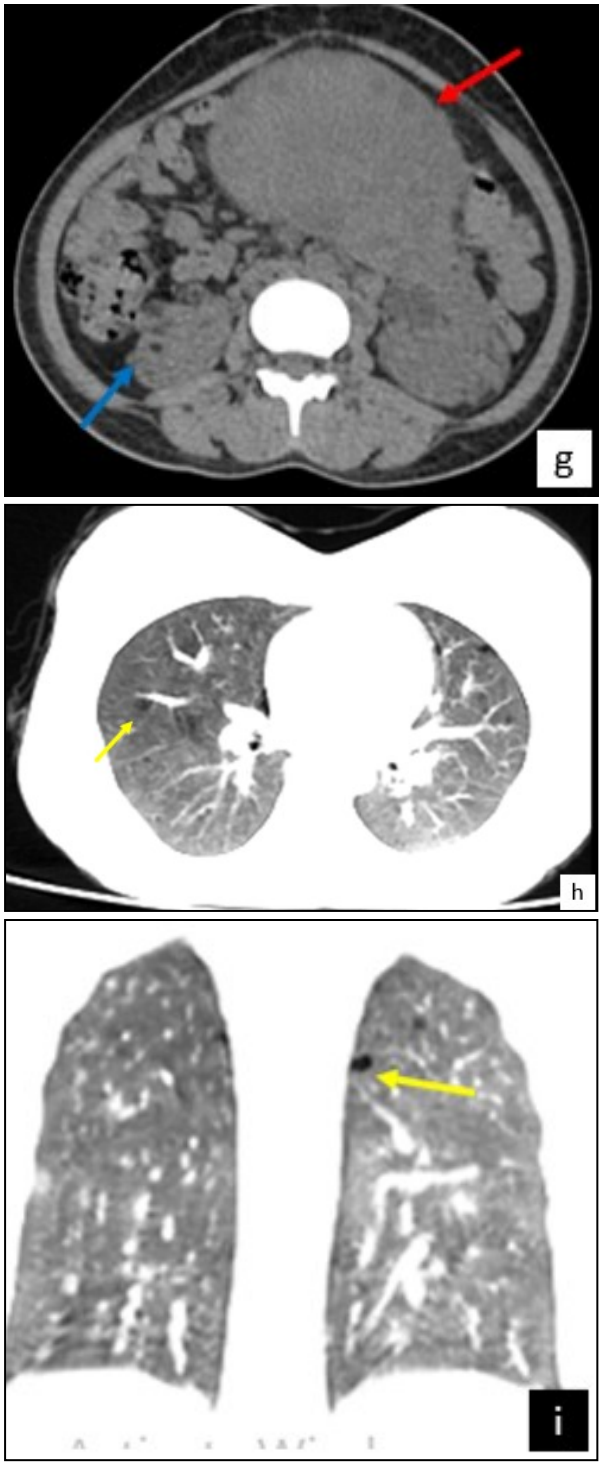

Fig. 3 a, b) – MRI images showing large T2 heterointense solid lesion measuring 12 x 17 x 21 cm arising from left kidney showing (red arrow) **c, d)** - DWI images showing peripheral diffusion restriction (red arrow) and **e)** – Gradient image showing few internal gradient blooming (red arrow) **f)** - with peripheral contrast enhancement and central non enhancing areas (red arrow) **g)** – CT image showing large lesion with internal fat densities in left kidney (red arrow) and a smaller lesion (blue arrow) in right kidney, **h, i)** – CT lung showing diffuse ground glass opacities with few scattered thin walled cysts in upper lobes (yellow arrow), **j)** – CT brain showing multiple calcified subependymal nodules

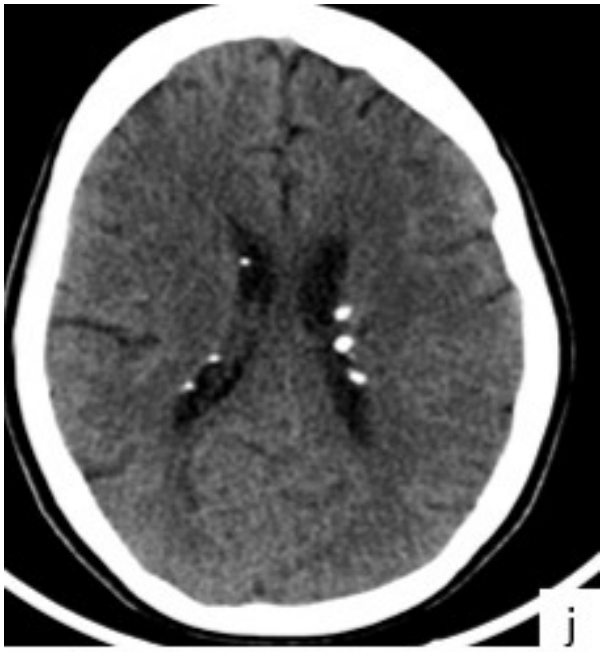

Case 4

An 18-year-old male presented to the dermatology clinic with multiple facial lesions of cosmetic concern. Dermatological evaluation revealed numerous bilaterally symmetrical facial angiofibromas (Fig. 4a) distributed across the cheeks, nasolabial folds, and chin. Additional findings included multiple hypo-pigmented macules—commonly referred to as “ash leaf” spots—over the lower back and upper limbs (Fig. 4b-c).

Given the constellation of cutaneous features suggestive of a phakomatosis, neuroimaging and abdominal imaging were pursued. MRI of the brain demonstrated a cortical tuber in right parietal region and multiple enhancing subependymal nodules along the walls of the lateral ventricles, appearing heterointense on T2-weighted sequences, with a few showing susceptibility on gradient imaging. Notably, a dominant lesion greater than 1 cm in diameter, located adjacent to the foramen of Monro, was identified and interpreted as a SEGA (Fig. 4d-g).

Abdominal CT revealed multiple bilateral renal AMLs, along with incidental sclerotic bone lesions in the dorsolumbar vertebrae (Fig. 4h-i). With the presence of five major diagnostic criteria—including dermatological, neurological, and renal findings—the diagnosis of TSC was unequivocally established.

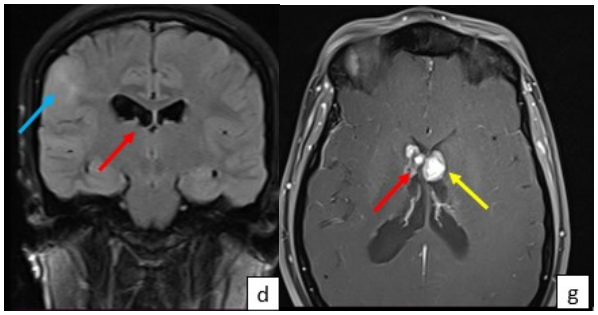

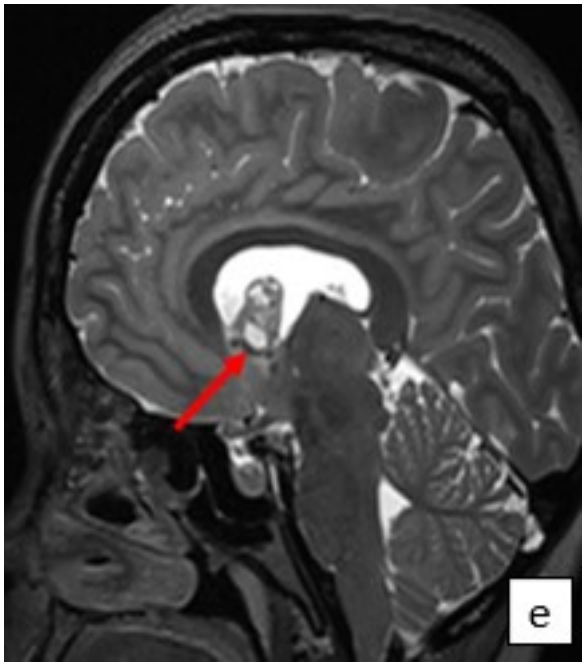

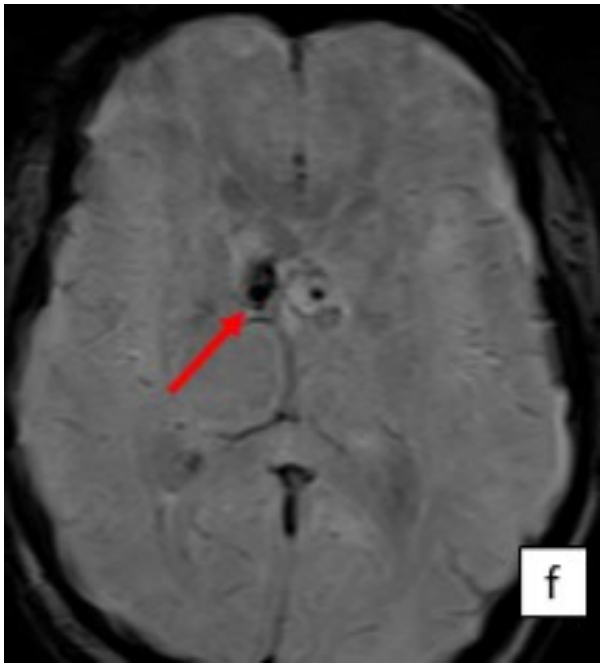

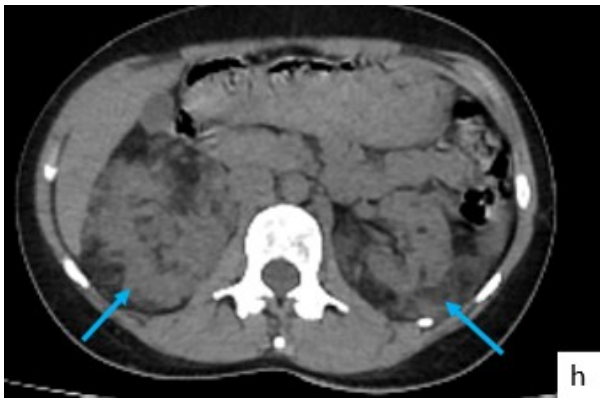

Fig. 4 a) – Clinical image of the patient showing multiple facial angiofibromas (red arrow) **b, c)** – Hypomelanotic macules noted in lower back and upper arms (red arrow) and **d)** – MRI Flair image showing cortical tubers in right parietal region (blue arrow) and subependymal nodules (red arrow) **e)** – T2 heterointense subependymal nodules noted with **f)** – few showing gradient blooming indicating calcification (red arrow) **g)** – Few subependymal nodules showing contrast enhancement (red arrow) and a large lesion consistent with SEGA (yellow arrow) noted, **h)** – CT abdomen showing bilateral renal AMLs (blue arrows), **i)** – CT bone window showing bone islands (green arrow).

Discussion

TSC is an uncommon genetic disorder characterized by diverse manifestations and a tendency for hamartomatous growth in many organs (6).

Depending on the organ of involvement, the patient presents with a wide range of clinical symptoms. Consequently, the 2012 International TSC Consensus Conference established revised diagnostic criteria, differentiating between major and minor features. A definitive diagnosis necessitates the presence of two major features or one major feature in conjunction with two minor features (7). Significantly, most of the major features can be discerned by imaging, underscoring the radiologist's essential and prominent function in the diagnosis process.

Cutaneous lesions frequently act as the initial indicator in the diagnosis of TSC, particularly in paediatric and teenage population. Hypomelanotic macules (90%), face angiofibromas (75%), shagreen patches (30%), and ungual fibromas are established dermatological manifestations (8). In Case 4, the occurrence of many angiofibromas and hypo-pigmented macules triggered imaging referrals and subsequent verification of systemic involvement. These lesions facilitate diagnosis, enable genetic counseling, and initiate screening for at-risk relatives.

Neurological involvement occurs in more than 90% of patients and represents the earliest clinical manifestation, especially in the form of seizures (9). The classic triad observed on imaging includes cortical tubers, SENs, and SEGA. Cortical tubers and/or subependymal nodules represent the predominant CNS manifestations, exhibiting a prevalence of 95-100% (10). Approximately 40% of cases also exhibit white matter lesions like radial migration lines (RML) (11).

Cortical tubers are hyperintense lesions on T2/FLAIR imaging within the cerebral cortex, which act as epileptogenic foci. SEGAs commonly develop adjacent to the foramen of Monro and can lead to obstructive hydrocephalus (12). In our series, two patients exhibited SEGAs, each exceeding 1 cm in size and displaying avid enhancement, aligning with established diagnostic criteria. SEN typically manifests on the ependymal surface of the lateral ventricles and exhibits a propensity for calcification over time. The possibility of SENs developing into SEGAs, especially in adolescence and early adulthood, highlights the significance of serial CNS imaging.

Renal symptoms are the second most prevalent findings in TSC. Approximately 20% of people with renal AML are identified with TSC, whereas 80% of individuals with TSC present with renal AMLs (13). AMLs are frequently large, bilateral, and multiple in the context of TSC. Cases 1 and 3 revealed substantial bilateral AMLs, accompanied by indications of hemorrhagic consequences and intratumoral aneurysms. AMLs exceeding 4 cm or exhibiting intratumoral aneurysms more than 5 mm are deemed at elevated risk for bleeding and may qualify for

Table 1. - Major and minor features for TSC diagnosis according to the revised clinical diagnostic criteria in the second "International Tuberous Sclerosis Complex Consensus Conference" held in Washington, DC, in 2012. TSC-1, tuberous sclerosis complex-1, TSC-2, tuberous sclerosis complex-2.

Major features	Minor features	Diagnosis
1. Hypomelanotic macules (3 or more and each ≥5 mm in diameter.) 2. Angiofibromas (3 or more) or fibrous cephalic plaque 3. Ungual fibromas (2 or more) 4. Shagreen patch 5. Multiple retinal hamartomas 6. Cortical dysplasias include tubers and radial migration lines of cerebral white matter. 7. subependymal nodules (SENs) 8. Subependymal giant cell astrocytoma (SEGA) 9. Cardiac rhabdomyoma 10. Lymphangioleiomyomatosis (LAM) 11. Angiomyolipomas (AML) (2 or more)	1. Confetti skin lesions 2. Dental enamel pits (More than 3) 3. Intraoral fibromas (2 or more) 4. Retinal achromic patch 5. Multiple renal cysts 6. Nonrenal hamartomas.	Diagnosis of definitive TSC requires one of the following: 1. Identification of either a TSC1 or TSC2 pathogenic mutation in DNA from normal tissue 2. Two major features 3. One major + at least two minor features.

embolization or mTOR treatment (14). TSC-associated AML typically manifest at a younger age and exhibit more rapid progression than sporadic variants. Other infrequent renal symptoms encompass bilateral multiple renal cysts, present in approximately 18-53% of cases, and clear cell renal cell carcinoma (RCC), observed in about 2-3% of instances (15).

Pulmonary involvement, predominantly manifesting as lymphangioleiomyomatosis (LAM), is an acknowledged characteristic of TSC, affecting approximately 26 to 39% of women with the condition (16). LAM is distinguished by diffuse, thin-walled cysts shown on high-resolution CT, frequently associated with ground-glass opacities or chylous effusions.

Case 3 has characteristic symptoms of LAM, stressing the necessity for chest imaging in asymptomatic adult female patients with TSC, due to the likelihood for spontaneous pneumothorax. LAM may sometimes manifest sporadically, necessitating additional major features for a conclusive diagnosis of TSC. Additional uncommon thoracic conditions encompass multifocal micronodular pneumocyte hyperplasia (MMPH) and clear cell sugar tumor (CCST) of the lung (13).

The principal cardiac manifestation of TSC is cardiac rhabdomyomas, which are the most often identified lesions in utero or in newborns. It manifests in approximately 70% of children, with the majority regressing during childhood. They are typically asymptomatic but can induce deadly arrhythmias, necessitating resection (17).

Skeletal involvement, although frequently incidental, includes sclerotic bone lesions, especially inside the axial skeleton (18).
Although asymptomatic, their existence, as observed in Cases 2 & 4, reinforces the diagnosis and may function as minor or ancillary criteria when the clinical presentation is ambiguous. Additional abdominal manifestations include hepatic angiomyolipomas, splenic hamartomas, and colorectal polyps in a minor percentage of TSC individuals (18).

The management of TSC is multidisciplinary and increasingly influenced by imaging techniques. The introduction of mTOR inhibitors, such as Everolimus, has transformed the treatment of TSC-associated SEGAs and AMLs (19). Serial imaging is essential for evaluating progression, guiding treatment response, and monitoring complications,

thereby requiring precise baseline imaging and subsequent measurements. In summary, imaging serves as cornerstone in the assessment and management of TSC.

Conclusion

This case series emphasizes the diverse radiological manifestations of TSC, highlighting the necessity of a thorough, cross-sectional imaging strategy—especially in individuals exhibiting apparently isolated symptoms. Prompt recognition of distinctive lesions, such as SEGAs, renal angiomyolipomas, and pulmonary cysts, not only enhances rapid diagnosis but also directs clinical judgements for surgical or medical interventions. Radiologists must be attentive to subtle diagnostic imaging clues, since these may be crucial in identifying a potentially overlooked multisystem disorder.

Correspondence to:
Thiagarajan Veerappan
Barnard Institute of Radiology, Madras Medical College, Chennai, Tamil Nadu, India

Declarations

Consent for publication: The author clarifies that written informed consent was obtained and the anonymity of the patient was ensured. This study submitted to Swiss J. Rad. Nucl. Med. has been conducted in accordance with the Declaration of Helsinki and according to requirements of all applicable local and international standards. All authors contributed to the conception and design of the manuscript, participated in drafting and revising the content critically for important intellectual input, and approved the final version for publication. Each author agrees to be accountable for all aspects of the work, ensuring its accuracy and integrity.
Competing interests: None.
Funding: No funding was required for this study.

Conflict of interest:

The authors declare that there were no conflicts of interest within the meaning of the recommendations of the International Committee of Medical Journal Editors when the article was written.

Disclaimer/Publisher's Note:

The statements, opinions and data contained in all publications are solely those of the individual author(s) and contributor(s) and not of Swiss J. Radiol. Nucl. Med. and/or the editor(s). Swiss J. Radiol. Nucl. Med. and/or the editor(s) disclaim responsibility for any injury to people or property resulting from any ideas, methods, instructions or products referred to in the content.

License Policy:

SJORANM-LinkedIn:

Check out our journal's LinkedIn profile with over 11K registered followers from the Radiologic & Nuclear Medicine Imaging field.

References

1. Domínguez-Valdez LF, Hernández-Utrera JE, Chávez-Sánchez IN, et al. Late diagnosis of tuberous sclerosis: a case report. Oxf Med Case Reports. 2023;2023(4):omad029. Published 2023 Apr 20. https://doi.org/10.1093/omcr/omad029

2. Dzefi-Tettey K, Edzie EK, Gorleku P, Piersson AD, Cudjoe O. Tuberous Sclerosis: A Case Report and Review of the Literature. Cureus. 2021;13(1): e12481. Published 2021 Jan 4. https://doi.org/10.7759/cureus.12481

3. Cao Y, Zhang H, Wang F, Zhu D, Liao M. Case Report Radiological appearance of tuberous sclerosis complex: a case report and review of literature. Int J Clin Exp Med. 2017;10(5):8282- 8287. https://e-century.us/files/ijcem/10/5/ijcem0050976.pdf

4. Manoukian SB, Kowal DJ. Comprehensive imaging manifestations of tuberous sclerosis. AJR Am J Roentgenol. 2015;204(5): 933-943. https://doi.org/10.2214/AJR.13.12235

5. Alshoabi SA, Hamid AM, Alhazmi FH, et al. Diagnostic features of tuberous sclerosis complex: case report and literature review. Quant Imaging Med Surg. 2022;12(1):846-861. https://doi.org/10.21037/qims-21-412

6. Kharrazi MH, Haghighatkhah HR, Noori M, Taheri MS. Intracranial Manifestations of Tuberous Sclerosis: A Pictorial Essay. Iranian Journal of Radiology. 2008;5(4):221-230. https://brieflands.com/journals/ijradiology/articles/79011.pdf

7. Gupta P, Kukreja R, Mital M, Rathee N. A case series of tuberous sclerosis complex: Clinico-radiological study and review of the literature. West African Journal of Radiology. 2017;24(1):109. https://doi.org/10.4103/1115-3474.198155

8. Umeoka S, Koyama T, Miki Y, Akai M, Tsutsui K, Togashi K. Pictorial review of tuberous sclerosis in various organs. Radiographics. 2008;28(7): e32. https://doi.org/10.1148/rg.e32

9. Stein JR, Reidman DA. Imaging Manifestations of a Subependymal Giant Cell Astrocytoma in Tuberous Sclerosis. Case Rep Radiol. 2016;2016:3750 450.https://doi.org/10.1155/2016/3750450

10. Passeri HR, Reis F, Luciano, Chwal BC, Duarte JÁ. Imaging of central nervous system manifestations of Tuberous Sclerosis: a current pictorial review for an “old” disease. Brazilian Journal of Health Review. 2023;6(2):8127-8144. https://doi.org/10.34119/bjhrv6n2-294

11. Fujii H, Sato N, Kimura Y, et al. MR Imaging Detection of CNS Lesions in Tuberous Sclerosis Complex: The Usefulness of T1WI with Chemical Shift Selective Images. AJNR Am J Neuroradiol. 2022;43(8): 1202-1209. https://doi.org/10.3174/ajnr.A7573

12. Aden M, Fawzi MO, Prosser D, et al. Central nervous system manifestations of tuberous sclerosis complex: A single centre experience in Qatar. Saudi Med J. 2024;45(11):1245-1252. https://doi.org/10.15537/smj.2024.45.11.20240444

13. Radhakrishnan R, Verma S. Clinically relevant imaging in tuberous sclerosis. J Clin Imaging Sci. 2011;1:39. https://doi.org/10.4103/2156-7514.83230

14. Garg P, Sharma A, Rajani H, Choudhary AR, Meena R. Tuberous sclerosis complex: The critical role of the interventional radiologist in management. SA J Radiol. 2021;25(1):2034. Published 2021 Mar 30. https://doi.org/10.4102/sajr.v25i1.2034

15. Jawaid B, Qureshi AH, Ahmed N, Yaqoob N. Bilateral renal angiomyolipomas in tuberous sclerosis. African Journal of Urology. 2021;27(1). https://doi.org/10.1186/s12301-021-00161-x

16. Ritter DM, Fessler BK, Ebrahimi-Fakhari D, et al. Prevalence of thoracoabdominal imaging findings in tuberous sclerosis complex. Orphanet J Rare Dis. 2022;17(1):124. Published 2022 Mar 15. https://doi.org/10.1186/s13023-022-02277-x

17. von Ranke FM, Faria IM, Zanetti G, Hochhegger B, Souza AS Jr, Marchiori E. Imaging of tuberous sclerosis complex: a pictorial review. Radiol Bras. 2017;50(1): 48-54. https://doi.org/10.1590/0100-3984.2016.0020

18. Wang MX, Segaran N, Bhalla S, et al. Tuberous Sclerosis: Current Update. Radiographics. 2021;41(7): 1992-2010. https://doi.org/10.1148/rg.2021210103

19. Franz DN, Krueger DA. mTOR inhibitor therapy as a disease modifying therapy for tuberous sclerosis complex. Am J Med Genet C Semin Med Genet. 2018;178 (3):365–73. https://doi.org/10.1002/ajmg.c.31655